Development of a New Method for Manufacturing Iron Foam Using Gases Generated by Reduction of Iron Oxide

doi: 10.2320/matertrans.MRA2007127

Materials Transactions, Vol. 48, No. 11 (2007) pp. 2937 to 2944

Development of a New Method for Manufacturing Iron Foam Using Gases Generated by Reduction of Iron Oxide

Taichi Murakami[1], Kensuke Ohara[2,*], Takayuki Narushima[3] and Chiaki Ouchi[3]

[1]*Institute of Multidisciplinary Research for Advanced Materials, Tohoku University, Sendai 980-8577, Japan*
[2]*Department of Materials Science and Engineering, Undergraduate courses, Tohoku University, Sendai 980-8579, Japan*
[3]*Department of Materials Processing, Graduate School of Engineering, Tohoku University, Sendai 980-8579, Japan*

A new method for manufacturing iron foam using CO and CO_2 as foaming gases was studied. This method consists of three stages: (1) mixing powders of pure iron, graphite, and hematite; (2) preparing the precursor by cold pressing the mixed powders; and (3) foaming by heating the precursor at temperatures between the liquidus and solidus in the Fe–C binary system. Molten iron containing carbon is foamed by gases generated by a reduction reaction. Optimizations of both the composition of the precursor and the heating conditions are required to produce the iron foam with high porosity. It was found that the content and powder size of hematite in the precursor significantly affect the porosity and pore diameter of the iron foam. Iron foam with a porosity of 55% and average pore diameter of around 500 μm is obtained by heating the precursor of Fe-3.1 mass%C-1.0 mass%Fe_2O_3 at 1543 K. [doi:10.2320/matertrans.MRA2007127]

(Received June 7, 2007; Accepted August 9, 2007; Published September 28, 2007)

Keywords: *iron foam, reduction gas, precursor, foaming agent, porosity, hematite*

1. Introduction

Foamed metals and alloys, which include porous and cellular materials, have various functional properties and their density is significantly less than that of a dense metal. There are several methods for manufacturing foamed metals and alloys, such as foaming, powder metallurgy, and casting. Powder metallurgy is essentially based on the sintering of a green compact produced from powders or fibers.[1,2] In more advanced technologies, pores are created by the entrapment of gas contained in a powder compact,[3] by the use of space-holding filler materials or hollow spheres,[4] and by the foaming of metal powder slurries.[5] A typical method in use of casting enables to produce lotus-type porous metals.[6,7] Pores are formed by utilizing the solubility difference of a supersaturated gas between liquid and solid phases and are aligned in a particular direction by unidirectional solidification. On the other hand, in the foaming method that utilizes a liquid state, an injection gas or a gas-releasing foaming agent is used to foam a liquid metal. Aluminum foam, which is one of the most well known foamed metals,[8–15] is manufactured by two methods. One of the methods is direct foaming.[8–13] In this method, a small amount of calcium is added into molten aluminum to increase the viscosity, and molten aluminum is poured into a casting mold. Subsequently, it is stirred together with a foaming agent such as TiH_2; foaming then occurs in molten aluminum. Finally, the foamed molten alloy is cooled in the mold. The other method is indirect foaming.[14,15] In this method, a solid precursor is first prepared using uniformly dispersed mixed powders consisting of a metal and foaming agent. Then, the precursor is heated, and it expands and foams as the metal matrix melts. Aluminum foam with a density of 0.069–0.54 g/cm^3 is obtained by these methods, and it has high energy and sound absorbabilities. However, aluminum foam is very expensive, although it has excellent properties. Another drawback of aluminum foam is that it has low plateau strength in compression.[10] The strengthening of aluminum foam by alloying has been studied, since higher energy absorbability has been achieved by the development of high-strength metal foam.

For structural applications, iron and steel foam materials are much superior to aluminum foam due to their lower cost, higher strength, and better weldability. If iron foam with high porosity can be manufactured, then, similar to aluminum foam, it can be used as a lightweight and high-functional materials in applications such as transport vehicles, machines, and structural parts. The decomposition temperatures of foaming agents used for manufacturing metal foams must be near the liquidus line of the foamed materials. The decomposition temperature of TiH_2 used for foaming aluminum ranges from 723 to 873 K;[16] hence, TiH_2 cannot be utilized to foam molten iron due to the high melting point of iron. Therefore, a new foaming agent is required for steel and iron. There have been some reports on a method for manufacturing iron foam. Park *et al.* have reported a manufacturing method based on the powder metallurgy route and investigated the compression property of the iron foam with Fe-2.5%C (where the percentage sign indicates composition in mass%; this representation has been used throughout the paper) manufactured using the foaming agents $MgCO_3$ and $SrCO_3$.[17–20] The decomposition temperature of these foaming agents ranges from 1560 to 1580 K, which is close to the liquidus line of the Fe-2.5%C alloy. However, these foaming agents can be used to manufacture iron foam with a limited range of carbon content from 2% to 3%.

In this study, the authors investigated a new method for manufacturing iron foam by employing CO and CO_2 gases generated by the reduction reaction between iron oxide and carbonaceous materials as the foaming gases. Similar to conventional powder metallurgy, this method consists of three stages: powder-mixing, cold pressing, and heating to the temperature of the solid/liquid two-phase region.

*Undergraduate Student, Tohoku University, Present address: Toyo Seikan Kaisha, Ltd.

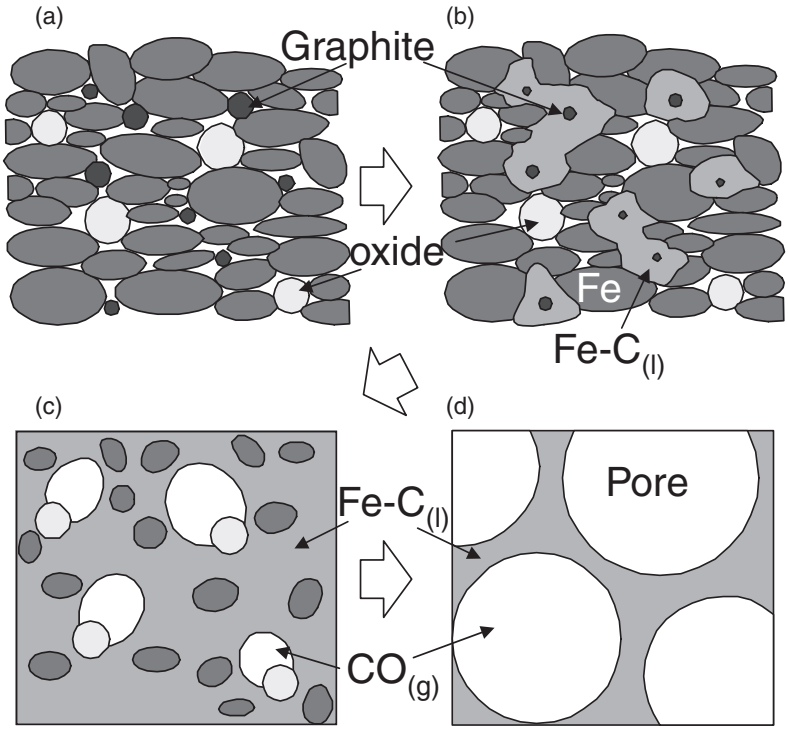

Fig. 1 Schematic diagram of foaming model using the precursor made by mixed powders of pure iron, graphite and hematite.

Figure 1 shows the schematic diagram of a foaming model using a precursor. The precursor is made by cold pressing mixed powders of pure iron, graphite, and iron oxide (hematite in this study); it is shown in Fig. 1(a). When the precursor is heated, molten iron is formed by the reaction between pure iron and graphite at a heating temperature beyond the eutectic temperature of 1426 K in the iron-carbon binary system. This state of constituents is shown in Fig. 1(b). As soon as the iron oxide encounters the molten iron containing carbon, the reduction reaction between the iron oxide and carbon proceeds abruptly. This phenomenon is shown in Fig. 1(c). This reaction is expressed by equation (1).

$$FeO_{X(s)} + \underline{C}_{(\text{in liquid})} = Fe_{(s)} + CO_{X(g)} \quad (1)$$

Large amounts of CO and CO_2 gases generated by this reaction foam the molten iron, as shown in Fig. 1(d). For manufacturing metal foams with high porosity by using this method, the optimization of the following two basic conditions is required: generation rate of foaming gas and the viscosity of the molten metal. The generation rate is primarily affected by the composition of the precursor and heating conditions. The molten metal with high viscosity should be formed in order to entrap the gas in the melt. In general, the viscosity of molten steel in the temperature range between the solidus and the liquidus, which is called the semisolid state, is higher than that of a single liquid phase. Therefore, this temperature range may be suitable to obtain an iron foam with high porosity.

In the present study, the precursor consisting of the mixed powders of pure iron, graphite, and hematite was prepared by cold pressing and the manufacture of iron foam by heating the precursor at a temperature between the liquidus and the solidus was attempted. The graphite and hematite contents of the precursor were varied in the ranges from 0.5% to 3.1% and from 0.01% to 4.0%, respectively. The powder size of hematite was also varied in the range from 1 to 20 μm. Furthermore, the effects of the heating conditions such as the heating rate, heating temperature, and heating time on the formation of iron foam or the porosity and pore size of iron foam were investigated.

2. Experimental Procedure

The raw materials used in this study were electrolytic pure iron, graphite, and hematite powders. The average powder sizes of the iron and graphite were 50 and 20 μm, respectively, and the average powder size of hematite was varied in the range from 1 to 20 μm. The composition ranges of graphite and hematite mixed with pure iron powder were from 0.5% to 3.1% and from 0.01% to 4.0%, respectively. The blended powders were compacted by uniaxial cold pressing at the stress of 180 MPa. The precursor was 14 mm in diameter, 10 mm in thickness, and 8 g in weight, and its surface was covered with a small amount of carbon paste to prevent decarburization during heating. The chemical compositions mentioned in the following section are not those obtained by the chemical analysis of iron foam but those of the precursor, which are calculated from the mixing ratio of various powders.

The precursor set on a steel disk was heated in Ar atmosphere using a high-frequency induction heating furnace. Two types of heating patterns were investigated, as shown in Fig. 2. In the first heating pattern shown in Fig. 2(a), the effects of the heating rate and graphite content of the precursor on foaming were examined. The heating rate

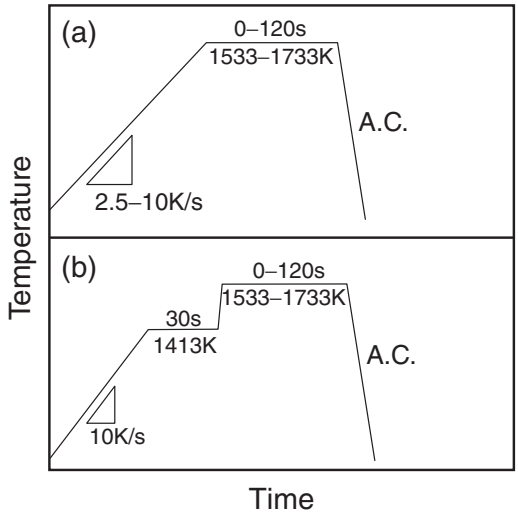

Fig. 2 Schematic diagram of (a) one step and (b) two steps heat patterns.

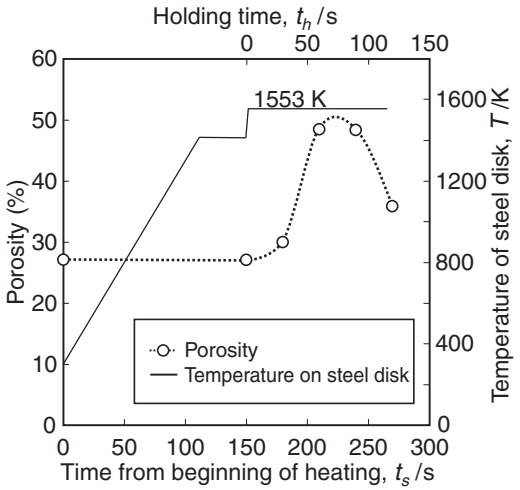

Fig. 3 Variation of the porosity with the heating time at 1553 K in use of the precursor Fe-3.1%C-1.0% Fe_2O_3. Average powder size of Fe_2O_3 is 1 μm.

and the heating temperature were varied in the ranges from 2.5 to 10 K/s and from 1533 to 1733 K, respectively. However, this heating pattern results in a large temperature distribution in the precursor during rapid heating. Therefore, the second heating pattern shown in Fig. 2(b) was adopted here, the precursor was heated to 1413 K at the heating rate of 10 K/s and was held at this temperature for 30 s in order to achieve a uniform temperature distribution. It was then heated at a heating rate over 30 K/s in the temperature range from 1533 to 1733 K. A Pt/Pt-13%Rh thermocouple used for temperature control was connected to the steel disk because it was impossible to connect it directly to the precursor. The temperature difference between the precursor and the steel disk was measured in advance, from which the temperature of the precursor was estimated. The temperature mentioned in the following section is the estimated temperature of the precursor, unless mentioned otherwise. The precursor was held at the specified temperature for the predetermined time. Subsequently, it was cooled in the furnace. The produced iron foam was cut along the cold-pressing direction and its cross section was obtained. The cross section of the iron foam was polished and etched by nital, and its macrostructures and microstructures were then observed by optical microscopy. The porosity and the average pore size of the foam were calculated using the area ratio of pore and the equivalent diameter because the volume ratio and average size of the pores could be evaluated using its area ratio and distribution, respectively.[21] Scion Image program—a software for image analysis[22] was used for the measurement of these value.

3. Results

3.1 Effects of heating conditions on foaming

Figure 3 shows the effect of the heating time at 1553 K on the porosity of the iron foam produced using the heating pattern of Fig. 2(b) for the steel disk and the precursor Fe-3.1%C-1.0%Fe_2O_3. The right vertical axis indicates the temperature of the steel disk, and the lower and upper horizontal axes show the total heating time from the beginning of heating and the holding time, respectively. The average powder size of hematite used was 1 μm. After preheating at 1413 K, the precursor was rapidly heated to 1553 K. However, at a very high heating rate, the actual temperature of the precursor could not follow the heating pattern. This is because the large number of micropores in the precursor (porosity: around 28%) tend to reduce its thermal conductivity; consequently, the actual heating rate inside the precursor may be lower than that in the steel disk. No change in the porosity was observed until the beginning of rapid heating. After the temperature of the precursor reaches 1553 K, the porosity increases abruptly with an extension of the holding time attained the peak value at the holding time of 80 s; and then decreased with a further extension of the holding time.

Bicolor images and microstructures of the cross section of the iron foam obtained by heating at 1553 K for various holding times are shown in Figs. 4 and 5, respectively. The white regions in the bicolor images indicate pores. When the heating temperature was just below the eutectic temperature, no change in the shape and the microstructure of the precursor was observed, and pure iron did not begin to melt due to its non-reaction with graphite. After holding for 30 s at 1553 K, the shape of the precursor does not change (Fig. 4(a)), and pure iron powders are deformed in a direction perpendicular to the cold-pressing direction (Fig. 5(a)). This result suggests that the eutectic reaction between iron and graphite did not proceed at this holding time. The results obtained for a holding time of 60 s are shown in Figs. 4(b) and 5(b). These figures reveal that the precursor expanded and iron foam with a pore size ranging from 0.1 to 5 mm was formed. The top surface of the foam has a convex shape, while the bottom surface is flat. The expansion due to foaming appeared to be suppressed in the bottom surface due to the dead weight of the precursor. The results obtained by an extension of the holding time to 90 s are shown in Figs. 4(c) and 5(c). Significantly, large pores are observed; it appears that they were formed by the coalescence of small pores. Therefore, the holding time is a very important parameter for producing iron foam with high porosity and

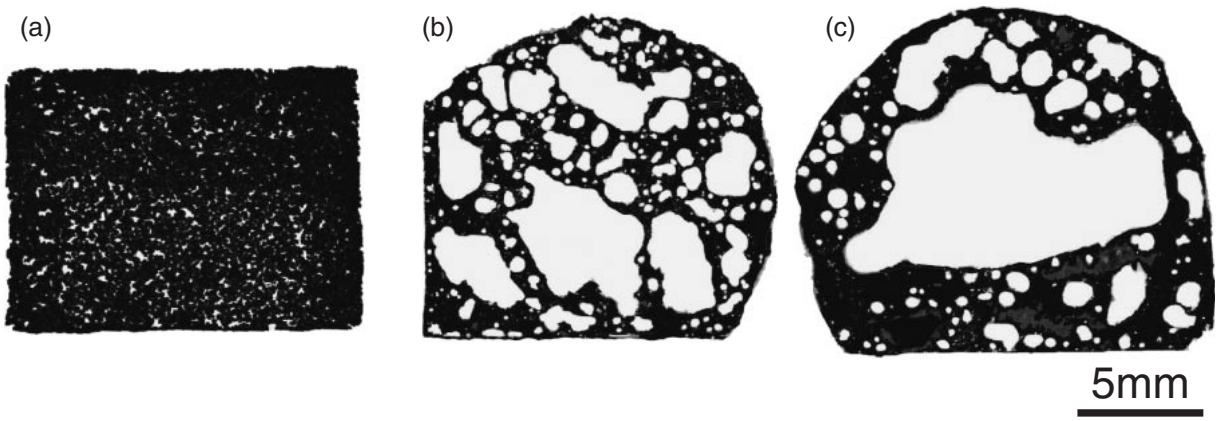

Fig. 4 Bicolor images of foams obtained by heating the precursor Fe-3.1%C-1.0% Fe_2O_3 at 1553 K for (a) 30, (b) 60 and (c) 90 s. Average powder size of Fe_2O_3 is 1 μm.

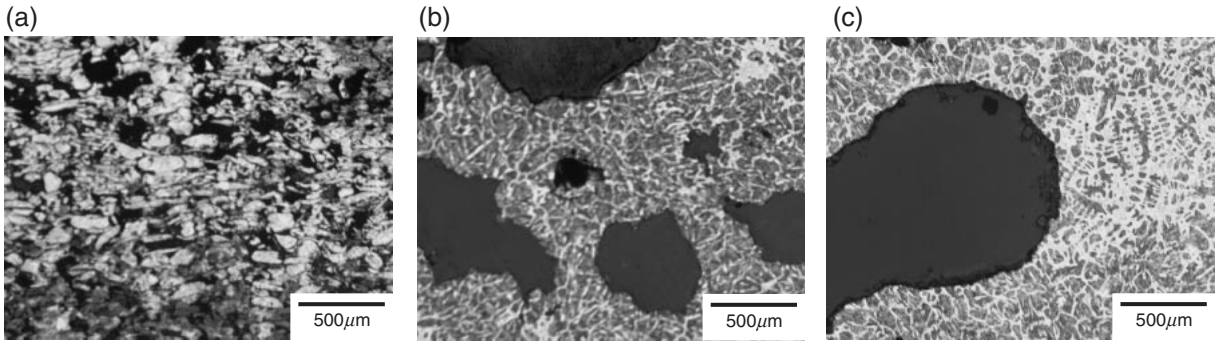

Fig. 5 Microstructures of foams obtained by heating the precursor Fe-3.1%C-1.0% Fe_2O_3 at 1553 K for (a) 30, (b) 60 and (c) 90 s. Average powder size of Fe_2O_3 is 1 μm.

uniform pore size. Iron foam with the highest porosity was obtained when the heating was terminated immediately after the onset of shrinkage of foamed iron. The holding time required for obtaining iron foam with the highest porosity varied due to several factors such as the composition of the precursor and the heating temperature; however, it mostly coincided with the holding time that yielded the largest expansion in the precursor. Therefore, all the results shown hereafter were obtained at this holding time.

Figure 6 shows the effect of the heating rate on the porosity of iron foam when the precursor Fe-3.1%C-1.0%Fe_2O_3 was heated at 1543 K. As mentioned earlier, the average powder size of the hematite used was 1 μm. The initial porosity of the precursor before heating was 28%, as noted before. Figure 7 shows the bicolor images of the iron foams obtained at various heating rates. At the heating rate of 2.5 K/s, the porosity was approximately 30%, which was almost the same as the micropore percentage of the precursor. In fact, the precursor scarcely expanded and the pores were very small. The relatively slow heating rate of 2.5 K/s may result in a decrease in the amount of foaming gas because the reduction reaction proceeded during slow heating. The relatively high values of the porosity, namely, 49% and 54%, were obtained at the heating rates of 3.3 and 5 K/s, respectively. Large pores are observed, which were formed by coalescence of small pores during foaming. The porosity decreases with a further increase in the heating rate, which may be explained as follows. The high heating rate enhanced

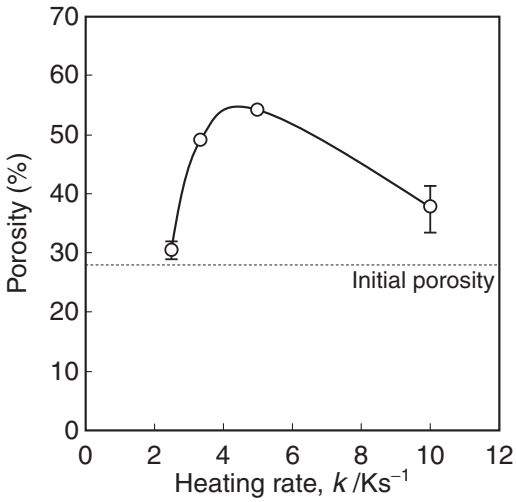

Fig. 6 Effect of heating rate on the porosity in iron foam obtained by heating the precursor Fe-3.1%C-1.0%Fe_2O_3 at 1543 K. Average powder size of Fe_2O_3 is 1 μm.

the nonuniform temperature distribution inside the precursor, where both the melted and unmelted regions were formed at the heating temperature. The foaming gas generated in the melted region could escape through the micropores in the unmelted region; consequently, the amount of gas available to foam molten iron reduced, resulting in a decrease in the porosity. These results suggest that it is important to optimize

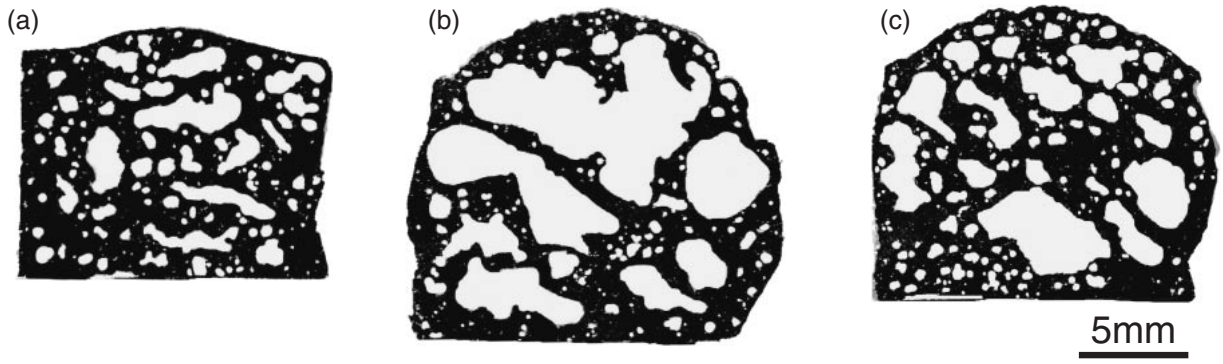

Fig. 7 Bicolor images of foams obtained by heating the precursor Fe-3.1%C-1.0% Fe_2O_3 at 1543 K at heating rates of (a) 2.5, (b) 3.3 and (c) 10 K s^{-1}. Average powder size of Fe_2O_3 is 1 μm.

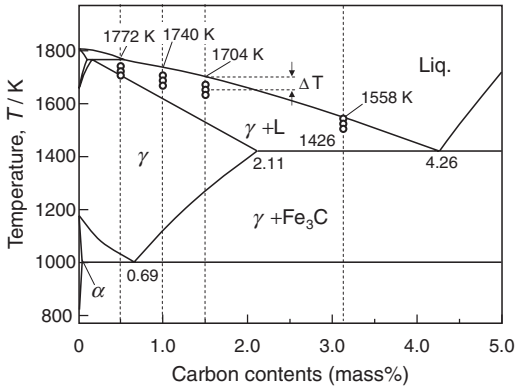

Fig. 8 Carbon contents and the range of heating temperature plotted on phase diagram of Fe-C system.

the melting rate of the precursor and the reduction rate of iron oxide for achieving high porosity, and the present result shows that the optimum heating rate ranges from 3.3 to 5 K/s.

3.2 Effect of graphite and hematite contents on foaming

In this study, the range of the heating temperature was varied depending on the graphite content of the precursor. Figure 8 shows the variation of the heating temperature range with carbon content on the Fe–C phase diagram. The temperature difference between the liquidus and the heating temperature is defined as ΔT. The effect of the carbon content on the formation of iron foam was investigated based on the first heating pattern shown in Fig. 2(a). The carbon contents shown in Fig. 8 indicate the graphite contents in the precursors but not the carbon contents in iron foams, because the latter was not measured, as noted before. Figures 9(a) and (b) show the effects of ΔT and the graphite content on the porosity of the iron foams, respectively. The amount of hematite and its average powder size were 1.0% and 1 μm, respectively. The porosity shown in Fig. 9(b) is the peak value for the corresponding graphite content shown in Fig. 9(a); therefore, the heating temperature is varied depending on the graphite content. The porosity varies depending on both the graphite content and the ΔT value. For given graphite content, the porosity first increases with ΔT, attains the peak value at a particular value of ΔT, and then decreases with a further increase in ΔT. The experimental error range of the porosity, which is shown in the data of 3.1% C in Fig. 9(a), increases with a decrease in ΔT. This appears to be caused by a decrease in the viscosity of the iron melt with an increase in the heating temperature. The value of ΔT yielding the peak value of the porosity increases with the

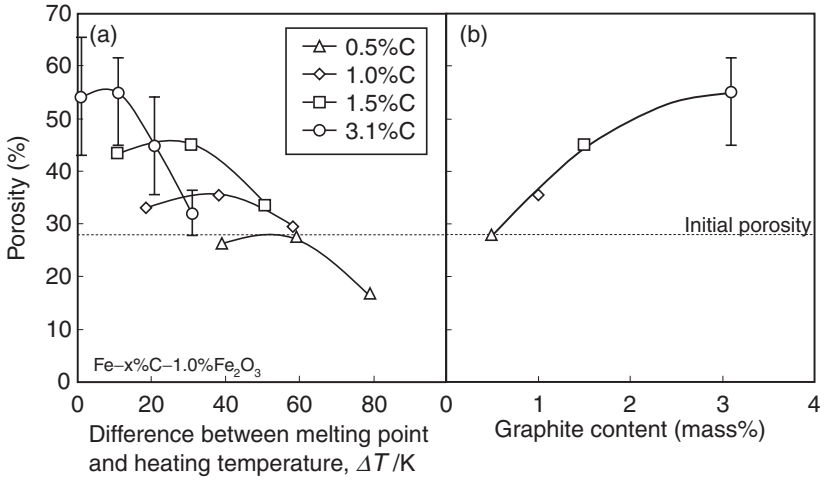

Fig. 9 Effects of (a) temperature difference, ΔT and (b) graphite contents on the porosity of foams obtained in precursors Fe-x%C-1.0%Fe_2O_3.

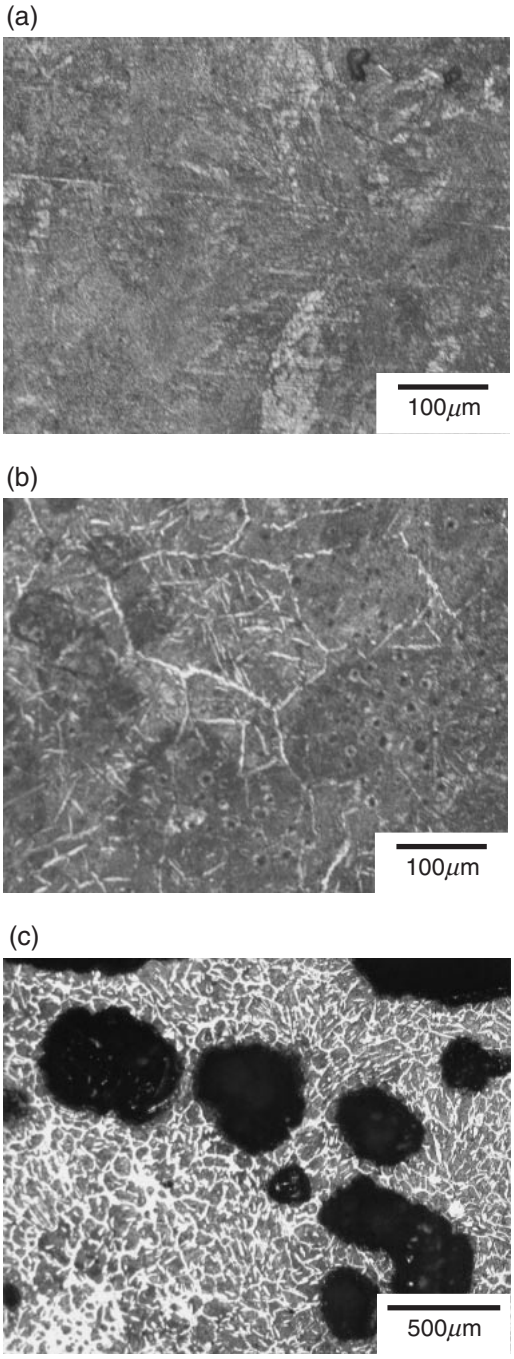

Fig. 10 Microstructures of foams obtained in Fe-x%C-1.0%Fe_2O_3 precursors. Carbon contents are (a) 1.0, (b) 1.5 and (c) 3.1%.

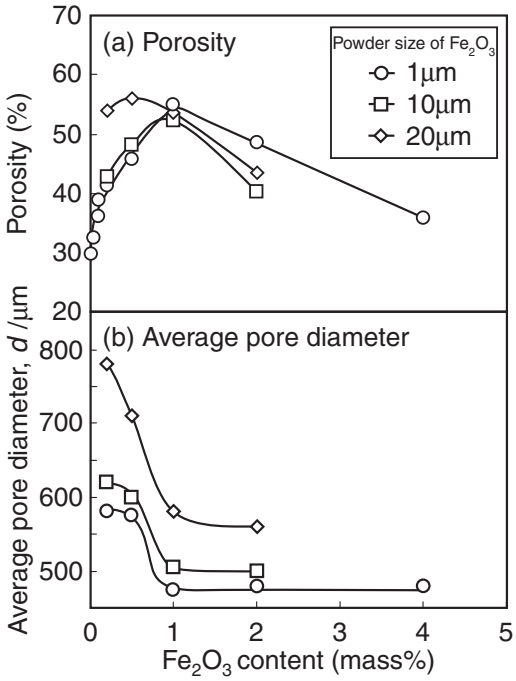

Fig. 11 Effects of Fe_2O_3 content and its powder size on the porosity and average pore diameter. The carbon content in the precursor is 3.1%.

decrease in the graphite content. The porosity increases with the graphite content, converging to a plateau value. It appears that the amount of foaming gas generated increases with increasing the graphite content, thereby enhancing the porosity. The variations in the microstructures of the foams with the graphite content in the precursor containing 1.0% Fe_2O_3 are shown in Fig. 10. The acicular cementite in the matrix formed by the eutectoid reaction and cementite formed along the austenitic grain boundary are observed in the iron foam with 1.5% C, and the amount of cementite decreases with decreasing the graphite content to 1.0%. A large amount of cementite is observed in 3.1% C iron foam as shown in Fig. 10(c).

Hematite is a key agent of gas generator used for the formation of the iron foam in this study. Therefore, the effects of the hematite content in the precursor and the powder size of hematite on the porosity and the pore size in the iron foam were systematically investigated under the constant graphite content of 3.1%, as shown in Fig. 11(a). For all the powder sizes of hematite, the porosity first increases with increasing the hematite content, attains a peak value, and then decreases. While the increase in the hematite content increases the amount of foaming gas and consequently the porosity, the excess amount of gas generated by the addition of an excess amount of the foaming agent appears to decrease the porosity. Further, the peak value of the porosity becomes slightly higher for a larger powder size of hematite. The effects of both—the hematite content in the precursor and the powder size of hematite—on the average pore diameter of the foams are shown in Fig. 11(b). The average pore diameter significantly decreases with increasing hematite content up to 1.0% and becomes constant thereafter. This variation in the pore size with the hematite content is not influenced by the powder size of hematite. However, the finer hematite powder results in the formation of finer pores in the foams. Consequently, the pore size of the foam can be controlled by the hematite content in the precursor and the powder size of hematite.

4. Discussion

4.1 Effect of the heating conditions on the formation of iron foam

An investigation of the effects of the heating rate, heating temperature, and time on the formation of the iron foam revealed that each of these parameters had an optimum range that would yield the iron foam with high porosity. These

optimum heating conditions appear to be associated with the optimum generation rate of the foaming gas. In the present method of manufacturing iron foam, two basic chemical processes occur during the heating of the precursor. The first process is the formation of melt containing carbon through the reaction between pure iron and graphite powders, and the second is the generation of the foaming gas by the reduction reaction between the melt and hematite powder.

The high heating rate and the short holding time at the heating temperature yielded the iron foam with a relatively low porosity. These heating conditions caused a large temperature distribution inside the precursor, which might have caused the formation of the melted and unmelted regions in the precursor. Therefore, the foaming gas generated at the interface between hematite and molten iron possibly escaped from the precursor, decreasing the amount of foaming gas available for the formation of the iron foam with a high porosity. A longer holding time at the heating temperature and a higher heating temperature also decreased the porosity. These heating conditions allowed the foaming gas to escape from molten iron, resulting in a decrease in the porosity. The low heating temperature also decreased the porosity, and this might be due to the non-formation of melt or the decrease in the rate of the reduction reaction. The other reason is associated with the viscosity of molten iron. The molten iron should have a high viscosity for preserving the foaming gas in the melt, and the viscosity may decrease with a decrease in the temperature between the solidus and the liquidus, which tends to decrease the preserved amount of foaming gas.

4.2 Effect of precursor composition on the pore formation

Achieving higher porosity is the most important criterion in the manufacture of iron foam, and as shown in Fig. 9, it was realized by increasing the graphite content in the precursor up to 3.1%. This inevitably decreases the foaming temperature because the liquidus in the Fe-C binary phase diagram decreases with an increase in the carbon content. The activity of carbon increases with a decrease in the temperature in the two-phase region. Therefore, the amount of the foaming gas increases with increasing the graphite content, as describe above. In addition, the liquid phase should have high viscosity to foam the melt using reducing gases because the foaming gas is apt to be trapped in the high-viscosity melt. The viscosity of the liquid phase increases with a decrease in the temperature. These factors appear to be responsible for the formation of the iron foam with high porosity using the precursor with high graphite content. Furthermore, the volume fraction of the liquid phase formed at the optimum foaming temperature increases with increasing the graphite content, as shown in Fig. 12, where the relationship between the volume fraction of the liquid phase and the graphite content in the precursor is shown. In this figure, the volume fraction of the liquid phase was obtained from the Fe-C binary phase diagram. For the precursor with lower graphite content, a low foaming temperature near the solidus was adopted from the viewpoint of viscosity. Consequently, the amount of the liquid phase available for the reaction with hematite increased with increasing the graphite content; this also contributed to the formation of high-porosity iron foam with high carbon content. However, it appears that the increase in the graphite content over 3.1% may be unfavorable to foaming due to a decrease in the viscosity, although no investigation was performed to confirm this.

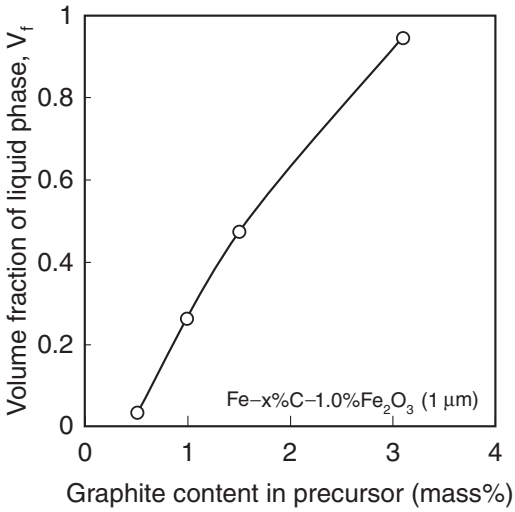

Fig. 12 Relation between graphite content in the precursor and the volume fraction of liquid phase at the optimum foaming temperature.

The other factor affecting the porosity of the foam is the hematite content. The highest porosity was obtained when the hematite content was around 0.5% to 1.0%, as shown in Fig. 11(a). The increase in the hematite content increases the amount of generated gases due to an increase in the contact area with the melt; consequently, the resulting iron foam has a high porosity. However, the addition of an excess amount of hematite may yield pores with a high pressure in the melt, which may bubble out from the melt. Therefore, the optimum hematite content must be determined. The hematite content and its powder size affected the average pore size of the foams, as shown in Fig. 11(b). The relation between the porosity and the pore size was analyzed using the data shown in Fig. 11. As shown in Fig. 13, this relation varies depending on the hematite content. When the hematite content is below 0.5%, the average pore diameter increases with increasing the porosity, and a finer hematite powder yields a higher porosity. When the hematite content is 1.0%, no relation between the pore diameter and porosity is observed, and a larger powder size of hematite yields a larger pore diameter, but has no influence on the porosity. When the hematite content is 2.0%, a higher porosity yields a smaller pore diameter; this trend is opposite to that observed for the hematite content below 0.5%. These results indicate that the pore size is affected by many factors including not only the composition of the precursor but also the heating conditions. As the optimization of the pore size and its distribution is important in the application of the iron foam as a structural or functional material, further investigation is required on factors that control the pore size.

The present method for manufacturing the iron foam utilizes foaming gases generated by the reduction reaction between carbon in molten iron and the hematite. Both CO

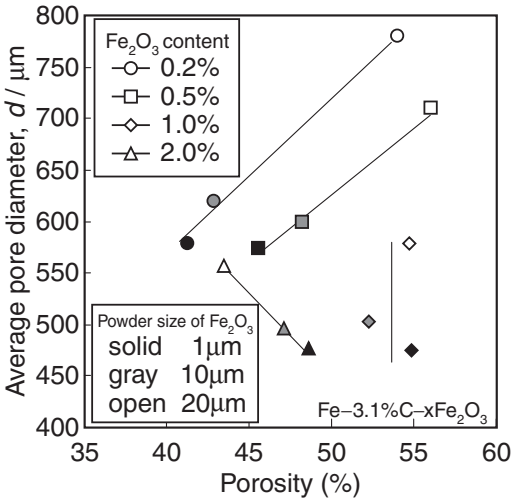

Fig. 13 Relation between the porosity and average pore diameter in the foams obtained in the precursor containing 3.1% C. Fe_2O_3 content and its powder size in the precursor are varied.

and CO_2 gases are possibly generated by this reaction. However, their actual amounts or ratios have not been investigated. It is essential to investigate and analyze the generated gases as well as conduct a chemical analysis of the iron foam, in particular, determine its carbon content. The highest porosity of the iron foam obtained in this study was around 55%, and the pore diameter ranged from 500 to 800 μm. This value of the porosity is insufficient for the industrial applications of iron foam. An increase in the viscosity of the melt may be required to produce the iron foam with a higher porosity. All these investigations would advance the present novel method for the manufacture of iron foam.

5. Conclusions

A new method for manufacturing iron foam based on powder metallurgy using pure iron, graphite, and hematite powders was studied. In this method, CO and CO_2 gases generated from hematite by the reduction reaction were utilized as foaming gases. The effects of the compositions of graphite and hematite and heating conditions on the production of the iron foam were investigated. Following results were obtained.

(1) It was found that the heating of the precursor at temperatures between the liquidus and solidus was required to foam molten iron, and the optimum heating rate to attain the highest porosity was from 3.3 to 5 K/s.

(2) The optimum temperature to manufacture the iron foam with high porosity varied with the graphite content of the precursor, and the porosity of the iron foam obtained at the optimum heating temperature increased with increasing the graphite content. The holding time at the optimum heating temperature also affected the porosity of the iron foam.

(3) The porosity of the iron foam increased with increasing the graphite content in the precursor, and the iron foam with the highest porosity of 55% and the average pore diameter of approximately 500 μm was obtained using the precursor with the composition of Fe-3.1%C-1.0%Fe_2O_3.

(4) The amount of hematite as well as its powder size significantly affected the porosity and pore size of the iron foam. The highest porosity of the iron foam was obtained using the precursor with a hematite content of approximately 1.0%.

Acknowledgment

This study was supported by The Shipbuilders' Association of Japan and the Ministry of Education, Culture, Sports, Science and Technology of Japan under grant number 18760558.

REFERENCES

1) I. H. Oh, N. Nomura and S. Hanada: Materials Transactions **43** (2002) 443–446.
2) O. Andersen: Metal Powder Report **54** (1999) 30–34.
3) D. M. Elzey and H. N. G. Wadley: Acta Materialia **49** (2001) 849–859.
4) O. Andersen, U. Waag, L. Schneider, G. Stephani and B. Kieback: Advanced Engineering Materials **2** (2000) 192–195.
5) T. Shimizu and K. Matsuzaki: Porous Metals and Metal Foaming Technology (JIMIC-4), ed. by H. Nakajima and N. Kanetake, (The Japan Institute of Metals, Japan, 2005) pp. 191–194.
6) H. Nakajima: Bulletin of ISIJ **6** (2001) 33–39.
7) S. K. Hyun and H. Nakajima: Materials Science and Engineering A **340** (2003) 258–264.
8) T. Mukai, H. Kanahashi, T. Miyoshi, M. Mabuchi, T. G. Nieh and K. Higashi: Scripta Materialia **40** (1999) 921–927.
9) T. Miyoshi, M. Itoh, S. Akiyama and A. Kitahara: Advanced Engineering Materials **2** (2000) 179–183.
10) S. Nishi, K. Makii, Y. Aruga, T. Hamada, J. Naito and T. Miyoshi: Kobe Steel Engineering reports **54** (2004) 89–94.
11) J. Banhart: Progress in Materials Science **46** (2001) 559–632.
12) D. Leitlmeier, H. P. Degischer and H. J. Flanke: Advanced Engineering Materials **4** (2002) 735–740.
13) C. C. Yang and H. Nakae: Journal of Materials Processing Technology **141** (2003) 202–206.
14) M. Kobashi, R. Sato and N. Kanetake: Porous Metals and Metal Foaming Technology (JIMIC-4), ed. by H. Nakajima and N. Kanetake, (The Japan Institute of Metals, Japan, 2005) pp. 169–172.
15) K. Kitazono, E. Sato and K. Kuribayashi: Scripta Mater. **50** (2004) 495–498.
16) A. R. Kennedy and V. H. Lopez: Mater. Sci. Eng. A **357** (2003) 258–263.
17) C. Park and S. R. Nutt: Mater. Sci. Eng. A **288** (2000) 111–118.
18) C. Park and S. R. Nutt: Mater. Sci. Eng. A **297** (2001) 62–68.
19) C. Park and S. R. Nutt: Mater. Sci. Eng. A **299** (2001) 68–74.
20) C. Park and S. R. Nutt: Mater. Sci. Eng. A **323** (2002) 358–366.
21) R. T. DeHoff and F. N. Rhines: *Quantitative Microscopy*, (McGraw-Hill Book Company, New York, 1968) pp. 1–8.
22) http://www.scioncorp.com/